

LncRNA CERS6-AS1, sponging miR-6838-5p, promotes proliferation and invasion in cervical carcinoma cells by upregulating FOXP2

Kun Yan², Chunyan Hu², Chen Liu², Guanghua Chu², Xinru Wang², Shuyun Ma³ and Long Li¹

¹Department of Gynecology and Obstetrics, the First Affiliated Hospital, Xi'an Jiaotong University,

Xi'an, China, ²The Second Department of Gynecology, Northwest Women and Children Hospital, Xi'an, China

and ³Department of Gynecology and Obstetrics, the First Affiliated Hospital, Xi'an Medical University, Xi'an, China

Summary. Cervical cancer (CC) is a common disease in women characterized by high recurrence rate. LncRNA ceramide synthase 6 antisense RNA 1 (CERS6-AS1) has been found to play a crucial role in the progression of breast cancer and pancreatic cancer. Nevertheless, the regulatory role of CERS6-AS1 in CC remains largely unclear. Here, we found that the expression of CERS6-AS1 was upregulated in CC tissues and cell lines compared with adjacent tissues and normal human cervical epithelial cells. CERS6-AS1 overexpression promoted proliferation and invasion, and inhibited apoptosis in CC cells, while silencing of CERS6-AS1 led to the opposite results. CERS6-AS1 was verified as a sponge of miR-6838-5p by RNA pull-down and luciferase reporter gene assays. Functional investigations revealed that CERS6-AS1 knockdown inhibited proliferation and invasion, and promoted apoptosis in CC cells, which was reversed by miR-6838-5p inhibitor. Furthermore, forkhead box P2 (FOXP2) was identified as a target for miR-6838-5p, and overexpression of miR-6838-5p decreased the expression level of FOXP2. Besides, CERS6-AS1 was able to sponge miR-6838-5p to accelerate CC cell proliferation and invasion and inhibited cell apoptosis through upregulating FOXP2 expression. In general, CERS6-AS1 was able to regulate CC cell proliferation, invasion and apoptosis by the miR-6838-5p/FOXP2 axis, which suggested that CERS6-AS1 may be a potential target for the treatment of CC.

Key words: Cervical cancer, lncRNA CERS6-AS1, miR-6838-5p, FOXP2

Introduction

Cervical cancer (CC) is a most common type of cancer in women and one of the top three cancers to affect women younger than 45. CC incidence ranks second among female cancers in the world, while it ranks first among female cancers in China (D'Oria et al., 2022). It is recently estimated that there are approximately 604,000 new CC patients with 342,000 deaths annually worldwide, among which approximately 85% new cases and 90% deaths occur in low- and middle-income countries (Bhatla et al., 2021). Although the survival rates of almost all malignant tumors, including CC, are improving all over the world, the rapidly increasing number of cases and deaths makes oncologists face a severe test (Caetano Dos Santos et al., 2022). Moreover, high incidence age of cervical carcinoma in situ is 30~35 years, and that of invasive carcinoma is 45~55 years old. In recent years, its incidence has a younger trend.

CC is a malignant tumor that occurs in the vaginal part of the uterus and cervical canal. Early cervical cancer often has no obvious symptoms and signs, and the cervix can be smooth or difficult to distinguish from ectopic cervical columnar epithelium. Patients with cervical canal type are prone to missed diagnosis or misdiagnosis due to normal cervical appearance. With the development of the disease, CC patients will have contact bleeding, vaginal discharge, frequent urination, urgency of urination, constipation, swelling and pain of lower limbs, and even ureteral obstruction, hydronephrosis and uremia, anemia, cachexia and other systemic failure symptoms (Volkova et al., 2021). Persistent infection of high-risk HPV (hrHPV) is the main risk factor of cervical cancer. More than 90% of cervical cancer is associated with hrHPV infection. However, compared with CC patients, hrHPV infection is more common in non-CC patients, and elimination of hrHPV can only be used as a means of prevention rather

Corresponding Author: Long Li, Department of Gynecology and Obstetrics, the First Affiliated Hospital, Xi'an Jiaotong University, Xi'an 710061, China. e-mail: longli_obs@126.com
www.hh.um.es. DOI: 10.14670/HH-18-555



than treatment of CC (Davies-Oliveira et al., 2021; Güzel et al., 2021). Consequently, it is urgent to explore deep pathogenesis and new therapeutic targets of CC.

Long noncoding RNAs (lncRNAs) are a class of RNA with lengths of more than 200 nucleotides and without protein-coding capacity. Increasing studies have confirmed that abnormal expression of lncRNAs is involved in multiple biological processes of cancers (Peng et al., 2017). For instance, lncRNA NEAT1 promotes migration and invasion in CC cells (Guo et al., 2018), while lncRNA MEG3 acts as a tumor suppressor to exert anti-cancer effect and inhibit tumor growth of CC (Zhang et al., 2016). lncRNA ceramide synthase 6-antisense 1 (CERS6-AS1) is a recently characterized lncRNA in a sequencing analysis exploring Alzheimer's disease (AD)-derived lncRNA-associated ceRNA network (Zhou et al., 2019). Soon after, CERS6-AS1 was found to be an important participant in mRNA-miRNA-lncRNA regulatory network linked to diagnosis and prognosis of hepatocellular carcinoma (Zhang and Lou, 2020). During the past three years, a few of studies have focused on the role of CERS6-AS1 and revealed it to be a proto-oncogene in several types of solid cancer. For example, in breast cancer, CERS6-AS1 was reported to interact with the RNA binding protein IGF2BP3 (insulin like growth factor II mRNA binding protein 3) to enhance the stability of CERS6 mRNA and promote breast cancer progression *in vitro* and *in vivo* (Bao et al., 2020). In colorectal and pancreatic cancers, CERS6-AS1 serves as a competitive endogenous RNA (ceRNA) by sponging miR-15a/b, miR-195-5p, miR-6838-5p and miR-217 to upregulate their targeting proto-oncogenes to promote cancer progression (Shen et al., 2021; Yun et al., 2021; Zhao et al., 2022). It is worth mentioning that CERS6-AS1 sponged miR-497 and then upregulated LIM and SH3 protein 1 to suppress ferroptosis and promote the growth of papillary thyroid cancer (Huang et al., 2022). However, its role and molecular mechanism in CC remain largely unexplored.

In the current study, we aim to reveal the exact function and molecular mechanism of CERS6-AS1 in regulating CC progression and to explore its potential as a potential therapeutic target for CC.

Materials and methods

Tissue samples

The CC tissues and adjacent normal tissues were collected from 30 CC patients who underwent radical resection at the First Affiliated Hospital, Xi'an Jiaotong University (Xi'an, China) from May 2017 to August 2019. All samples were cryopreserved at -80°C. No patient received any form of tumor treatment before collection. Informed consent was signed by each CC patient recruited in this study. All experiments were approved by the Ethics Committee of the First Affiliated Hospital, Xi'an Jiaotong University.

Cell culture

Human CC cell lines (HeLa, SiHa, C33A and CaSki) and normal human cervical epithelial cells (H8) were purchased from Cell Bank of the Chinese Academy of Sciences (Shanghai, China). All cells were cultured in Dulbecco's modified Eagle's medium (DMEM; Gibco; Thermo Fisher Scientific, Inc., Waltham, MA, USA) supplemented with 10% fetal bovine serum (FBS; Gibco, Grand Island, NY, USA) and 1% antibiotics in a humidified atmosphere of 5% CO₂ at 37°C.

Quantitative Real-Time Polymerase Chain Reaction (RT-qPCR)

Total RNA of cells and tissues was isolated with Trizol reagent (Invitrogen, Carlsbad, CA, USA) and reversely transcribed into cDNA using PrimeScript™ RT reagent Kit (Takara, Dalian, China). The ABI PRISM 7000 Fluorescent Quantitative PCR System (Applied Biosystems) was employed to progress the RT-qPCR with the following steps: 95°C for 10s followed by 40 cycles at 95°C for 5s, 60°C for 31s, and 72°C for 15s. The RT-qPCR reaction system was as follows: 2 μL of cDNA (150 ng/μL) was added to 10 μL of the 2× SYBR green PCR master mix with 0.4 μL of Taq polymerase enzyme (5 U/μL) (RiboBio, Guangzhou, China), 0.8 μL of each primer (10 mM) and 6 μL of ddH₂O to a total volume of 20 μL. The relative expression was determined by using the 2^{-ΔΔCt} method. The relative gene expression was normalized to glyceraldehyde 3-phosphate dehydrogenase (GAPDH) or U6 RNA. The sequences of the primers are as follows: CERS6-AS1 (forward: 5'-GCA GCC CAG CAG AAG TAG GA-3'; reverse: 5'-GAG CAT AGG GAA GCA ACT CTC AG-3'); miR-6838-5p (5'- GCA CTC CTG GAT GCC AAT CT-3'; reverse: 5'- CTC TAC AGC TAT ATT GCC AGC CAC-3'); FOXP2 (forward: 5'-AAG AAT GCA GTA CAT CAT AAT CTT AGC-3'; reverse: 5' - GCT AAG ATT ATG ATG TAC TGC ATT CTT -3'); GAPDH (forward: 5' -AGA AGG CTG GGG CTC ATT TG-3'; reverse: 5' -AGG GGC CAT CCA CAG TCT TC-3'); U6 forward (5'-CTC GCT TCG GCA GCA CA-3'; reverse: 5'-AAC GCT TCA CGA ATT GCG T-3').

Cell transfection

CERS6-AS1 overexpression plasmid and small interfering RNA (siRNA) (pcDNA-CERS6-AS1 and si-CERS6-AS1) or their negative controls (vector and scramble), miR-6838-5p mimic and its negative control (NC mimic), FOXP2 overexpression plasmid (pcDNA-FOXP2) and its negative control (vector) were provided by Ribobio (Guangzhou, China). HeLa and SiHa cells were transfected with 50 nM oligonucleotides or 2 μg of vector by using Lipofectamine 2000 (Invitrogen, Carlsbad, CA, USA) according to the manufacturer's instructions.

CERS6-AS1 promotes cervical carcinoma progression

Cell Counting Kit-8 (CCK-8) assay

Cell proliferation was measured using CCK-8 method in 96-well culture plates. The transfected HeLa and SiHa cells were placed on plates and grew at 37°C in a humidified atmosphere of 5% CO₂ for 24, 48 and 72h respectively. Then, 10 μL of CCK-8 solution (Invitrogen, Carlsbad, CA, USA) was added to each well. The mixture was incubated for 4h. The absorbance was measured at 450 nm using a microplate reader (Molecular devices, Shanghai, China).

Flow cytometry

HeLa and SiHa cells were seeded into six-well plates and cultured in a humidified atmosphere of 5% CO₂ at 37°C for 24h. Then, the cells were harvested by centrifugation and re-suspended with binding buffer (Beyotime, Shanghai, China). After that, the cells were stained with Annexin V-fluorescein isothiocyanate (FITC) and Propidium iodide (PI) (Beyotime) for 15 min on ice in a dark room. The fluorescence signals were measured by using Flow cytometer (BD Biosciences, USA).

Cell invasion assays

The invasion of HeLa and SiHa cells was detected using Transwell chambers with coated Matrigel (Corning Inc., Corning, NY, USA). 1×10⁴ cells were seeded into upper chambers containing the serum-free medium, while the lower chambers were added to medium containing 10% serum. After incubation at 37°C in a humidified atmosphere of 5% CO₂ for 24h, the lower chamber cells were fixed with 4% paraformaldehyde and stained with crystal violet, and the number of invasion cells were examined under an inverted microscope (Leica, Wetzlar, Germany). Cell invasion ability was represented as the percentage of cell invasion: invasive cells/total living cells.

3D invasion assay was also used for the invasion capacities of HeLa and SiHa cells. Briefly, the plasmid carrying fluorescent protein was transfected into the treated cells so that they could be sorted out by ultra-high speed flow cytometry later. The cells were cultured in CAwell600 High Throughput 3D Cellular Sphere Microarray (XiruiBio, Shenzhen, China) to obtain multicellular sphere. The mixture of the tumor multicellular sphere and type I collagen were added into the laser confocal culture dish, solidified, and cultured continuously. The tumor multicellular sphere extended, invaded and grew in type I collagen. When there was an obvious collective invasive cell group, a laser confocal microscope was used to bleach the tumor cells in the required specific area. Collagenase digestion, centrifugation and resuspension were applied to prepare cell suspension and flow cytometry sorting to obtain tumor cells in specific areas. Invasive areas were

calculated.

Western blotting

Total protein of cells was extracted by using RIPA lysis buffer (Beyotime, Shanghai, China) with protease inhibitor and examined by BCA Protein Assay Kit (Beyotime, Shanghai, China). 20 μg of proteins were isolated by 10% SDS-PAGE gels and then electro-transferred onto PVDF membranes. The membranes were closed with 5% non-fat milk and incubated with primary antibody at 4°C overnight. The primary antibodies are as follows: anti-FOXP2 (1:1000, ab16046, Abcam), anti-MMP2 (1:1000, ab92536, Abcam), anti-E-cadherin (1:1000, ab40772, Abcam) and anti-GAPDH (1:1000, ab9485, Abcam). The membranes were incubated with horseradish peroxidase-conjugated goat anti-rabbit immunoglobulin G (1:500, ab6721, Abcam) for 1 h at room temperature. Signals were visualized by Enhanced Chemiluminescence Western Blot Detection Kit (Amersham Pharmacia Biotech). The protein abundances were detected with a ChemiDoc XRS Imaging System (Bio-Rad). The gray value ratio of target protein to internal reference GAPDH was detected by Image J software (National Institutes of Health) to obtain the relative protein expression.

RNA pull-down assay

The bio-probe-NC, bio-miR-6838-5p-WT and bio-miR-6838-5p-MUT were synthesized and labeled using Biotin RNA Labeling Mix (Roche) and Sp6 RNA polymerase (Roche). The DNAs were treated with DNase I and purified with a RNeasy MiniKit (Qiagen, Hilden, Germany). The labeled RNA (1 μg) was heated in an RNA structure buffer (10 mM Tris pH 7.0, 0.1 mM KCl, 10 mM MgCl₂) to 95°C for 2 min, incubated on ice for 3 min, and then incubated at room temperature for 30 min to allow the formation of a secondary structure. Besides, HeLa and SiHa cells were lysed by cell lysis buffer (Sigma). Cell lysates were collected and incubated with streptavidin-agarose beads (Invitrogen) at 4°C for 1h. After RIP buffer washing, RT-qPCR was used to analyze the relationship between CERS6-AS1 and miR-6838-5p.

Luciferase reporter gene analysis

Through the Starbase database, we screened out miR-6838-5p for deep analysis and found the potential targeting relation of miR-6838-5p and CERS6-AS1. The binding sites of CERS6-AS1 were amplified and subcloned into the pmirGLO vectors (Promega) to construct CERS6-AS1 wild-type reporter (CERS6-AS1-WT) and mutated-isoform (CERS6-AS1-MUT) encompassing mutated binding site. The luciferase plasmids CERS6-AS1-WT and CERS6-AS1-MUT were

co-transfected with miR-6838-5p mimics or miR-6838-5p inhibitor into HeLa and SiHa cells. After 48h, the luciferase activity was analyzed by using the Dual-Luciferase Reporter Gene Assay System according to the manufacturer's instructions (Promega).

The targeting relation of miR-6838-5p and FOXP2 3'UTR were predicted using the database. The binding site of FOXP2 3'UTR was amplified and subcloned into the pmirGLO vectors (Promega) to construct FOXP2 3'UTR wild-type reporter (FOXP2-WT) and mutated-isoform (FOXP2-MUT) encompassing mutated binding site. The luciferase plasmids FOXP2-WT and FOXP2-MUT were co-transfected with miR-6838-5p mimics into HeLa and SiHa cells. After 48h, the luciferase activity was analyzed using the Dual-Luciferase Reporter Gene Assay System according to the manufacturer's instructions (Promega).

RNA immunoprecipitation (RIP) assay

EZ-Magna RIP RNA-binding protein immunoprecipitation kit (Millipore, USA) was used in RIP experiment. The transfected HeLa and SiHa cells were ruptured using RNA lysis buffer containing the protease and RNase inhibitors. Cell lysates were added to the RIP buffer containing the magnetic beads coated with anti-human argonaute 2 (Ago2) antibody (Millipore, USA) or IgG overnight. After washing three times, the beads were incubated with proteinase K. TRIzol reagent was used to isolate total RNA from the extracts. The co-precipitated RNAs were measured by RT-qPCR analysis.

Statistical analysis

Statistical analysis of experimental data was processed by using SPSS 23.0 (SPSS Inc, Chicago, IL). Data were expressed as mean \pm SD. Significance of the variance between two groups was determined by Student's t test. Significance of the variance among multiple groups was analyzed by ANOVA. $P < 0.05$ was considered statistically significant. All experiments were

performed three times.

Results

The expression of lncRNA CERS6-AS1 is upregulated in CC tissues and cell lines

To examine the role of CERS6-AS1 in CC, the expression of CERS6-AS1 was evaluated in CC tissues and adjacent tissues by RT-qPCR. The expression of CERS6-S1 in CC tissues was significantly upregulated compared with adjacent normal tissues (Fig. 1A). Additionally, RT-qPCR was also used to detect the CERS6-S1 expression level in CC cell lines. As expected, CERS6-S1 was highly expressed in C33A, HeLa, SiHa and CaSki cells compared to normal cervical epithelial cells (H8) (Fig. 1B).

lncRNA CERS6-AS1 promotes proliferation and inhibits apoptosis of CC cells

To examine the biological function of CERS6-AS1, we transfected CERS6-AS1 overexpression plasmid (pcDNA-CERS6-AS1) or CERS6-AS1 siRNA into HeLa and SiHa cells, respectively. RT-qPCR assay showed that overexpression of CERS6-AS1 could effectively increase CERS6-AS1 expression level in HeLa and SiHa cells compared with vector control, and silencing CERS6-AS1 could significantly downregulate the expression of CERS6-AS1 compared with scramble control (Fig. 2A). CCK-8 assay revealed that the proliferation ability of HeLa and SiHa cells was promoted by transfection with CERS6-AS1 overexpression plasmid and inhibited by transfection with CERS6-AS1 siRNA (Fig. 2B). Flow cytometry assay suggested that overexpression of CERS6-AS1 suppressed cell apoptosis, and knockdown of CERS6-AS1 induced cell apoptosis (Fig. 2C). Then, transwell assay and 3D cell invasion assay indicated that overexpression of CERS6-AS1 caused a marked increase in the number of invaded HeLa and SiHa cells,

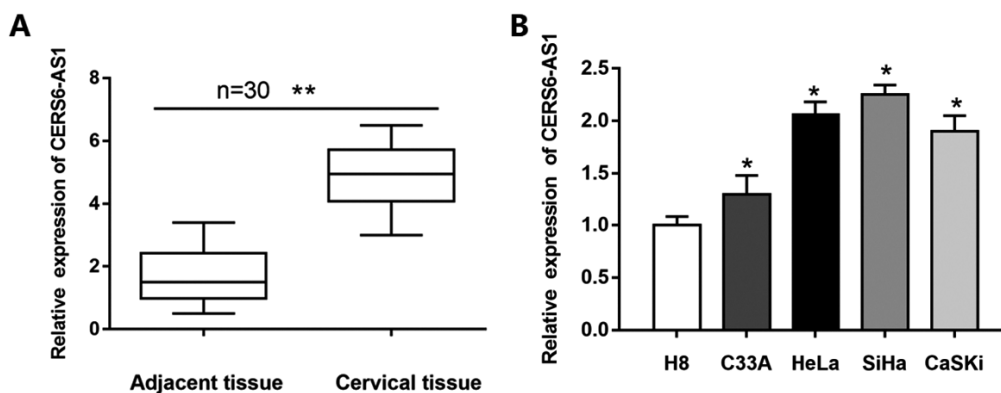


Fig. 1. The expression of CERS6-AS1 in CC tissues and cell lines. **A.** RT-qPCR was used to measure the expression level of CERS6-AS1 in CC tissues and adjacent tissues (n=30). **B.** RT-qPCR was used to measure the expression level of CERS6-AS1 in CC cell lines (C33A, SiHa, HeLa and CaSki) and normal cell line (H8). Data were expressed as mean \pm standard deviation with three replicates. ** $P < 0.01$ vs adjacent tissues (A), and * $P < 0.05$ vs normal human cervical epithelial cells (H8) (B).

CERS6-AS1 promotes cervical carcinoma progression

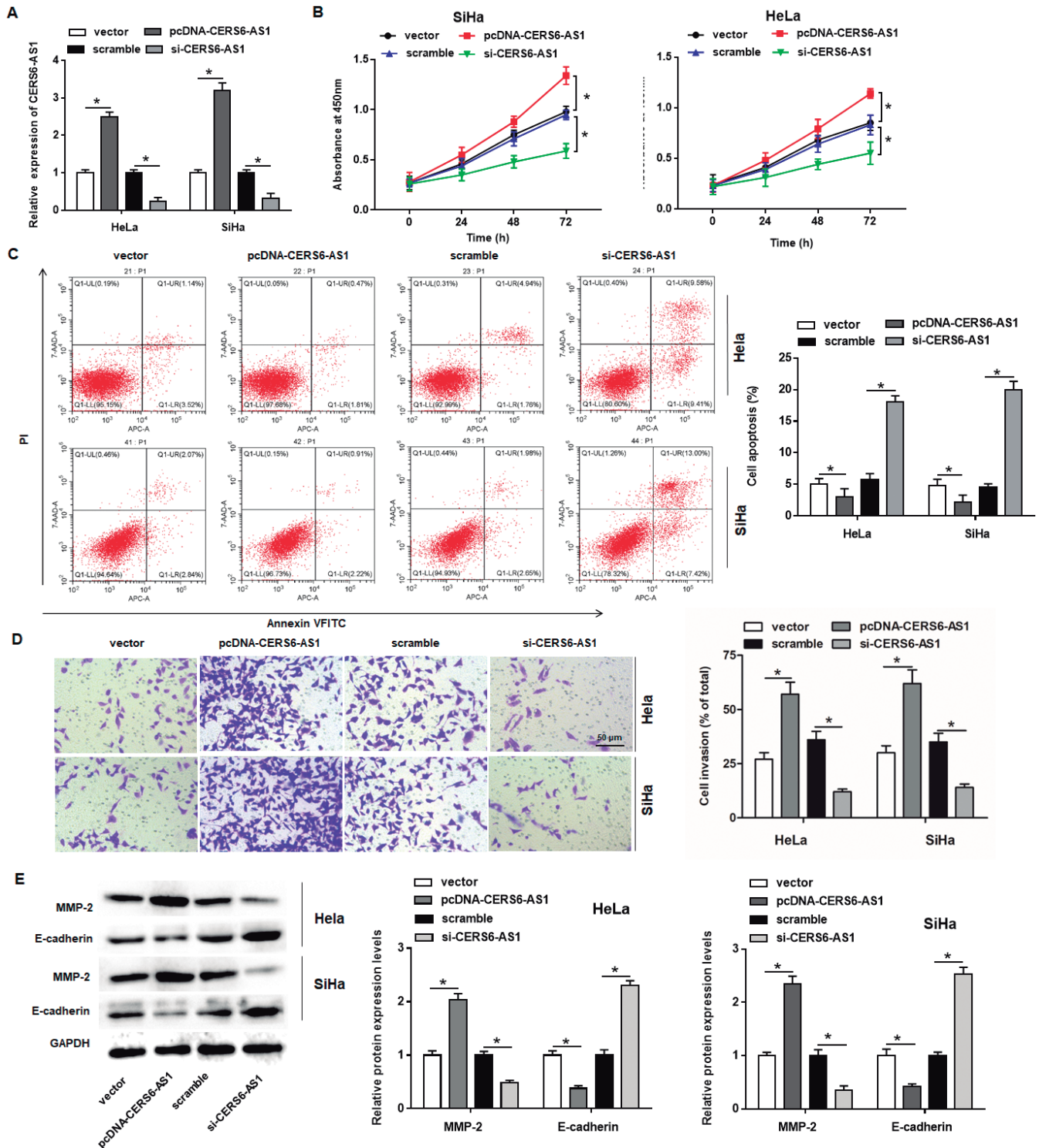


Fig. 2. Effects of CERS6-AS1 overexpression on the progression of CC cells. HeLa and SiHa cells were transfected with CERS6-AS1 overexpression plasmid or CERS6-AS1 siRNA, and incubated for 24h. **A.** The expression of CERS6-AS1 was examined by RT-qPCR. **B.** The proliferation ability of transfected cells was detected by CCK-8 assay. **C.** Apoptosis ability of transfected cells was measured by flow cytometry assay. **D.** Transwell assay showed the invasion ability of transfected cells. **E.** The expression of MMP-2 and E-cadherin was detected by Western blot assay. Data were expressed as mean \pm standard deviation with three replicates. * $P < 0.05$, vs vector group or scramble group.

and CERS6-AS1 silencing led to the opposite results (Fig. 2D, Fig. 3). The metastasis-related protein (MMP-2) and EMT-related protein expression levels (E-cadherin) were detected by Western blot assay. The results showed that CERS6-AS1 overexpression increased the protein level of MMP-2 and reduced the protein level of E-cadherin. On the contrary, MMP-2 expression was significantly decreased and E-cadherin expression was remarkably augmented in CERS6-AS1 siRNA group (Fig. 2E). Therefore, the above results illustrated that CERS6-AS1 might act as an oncogene to promote CC cell proliferation and invasion.

CERS6-AS1 sponges miR-6838-5p in CC

We explored differentially expressed miRNAs in non-treated cervical cancer cells (HeLa or SiHa) and cervical cancer cells treated with several anti-tumor extracted components from traditional Chinese Medicine (including emodin, curcumin and Ginsenoside). Shared miRNAs were screened and the results showed that miR-7110-5p and miR-4298 were the only two miRNAs that are higher in non-treated cells compared with all the treated cell groups, while miR-6838-5p/3p were the only two miRNAs that are lower in non-treated cells compared with all the treated cell groups (Fig. 4). Moreover, we also found that miR-6838-5p was remarkably downregulated in C33A, HeLa, SiHa and CaSki cells (Fig. 5A). Through Starbase V3.0 software, we found the binding sites of miR-6838-5p on CERS6-AS1 (Fig. 5B). In addition, RNA pull-down assay showed that CERS6-AS1 was significantly increased in the bio-miR-6838-5p-WT group compared with the bio-probe-NC group in HeLa and SiHa cells, while no

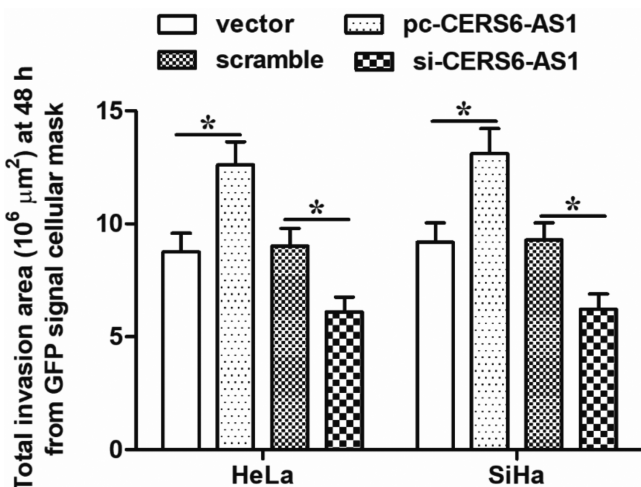


Fig. 3. 3D cell invasion assay was used to evaluate the effect of CERS6-AS1 on overall invasion ability of CC cells. HeLa and SiHa cells were transfected with CERS6-AS1 overexpression plasmid or CERS6-AS1 siRNA. 3D cell invasion assay was used to evaluate the overall invasion ability of CC cells. N=4, *P<0.05

significant difference was observed in the bio-miR-6838-5p-MUT (Fig. 5C). Through the luciferase reporter gene assay, we further found that the luciferase activity of CERS6-AS1-WT was effectively decreased by miR-6838-5p overexpression, but markedly elevated by miR-6838-5p inhibition (Fig. 5D). Furthermore, to assess whether the expression of miR-6838-5p was regulated by CERS6-AS1, we transfected CERS6-AS1 overexpression plasmid into HeLa and SiHa cells. The results reflected that miR-6838-5p expression was restrained by CERS6-AS1 overexpression. (Fig. 5E). These results demonstrated that CERS6-AS1 regulated miR-6838-3p expression in CC cells.

MiR-6838-5p inhibitor reverses CERS6-AS1-knockdown-mediated effect on proliferation and apoptosis in CC cells

Given the relationship between miR-6838-5p and CERS6-AS1, it is necessary to investigate the effect of miR-6838-5p on the development of CC. The expression of miR-6838-5p was upregulated after silencing CERS6-AS1 in HeLa and SiHa cells (Fig. 6A). CCK-8 and transwell assays showed that introduction of miR-6838-5p inhibitor reversed the inhibitory effect of CERS6-AS1 silencing on cell proliferation and invasion in HeLa and SiHa cells (Fig. 6B,D). Flow cytometry assay also

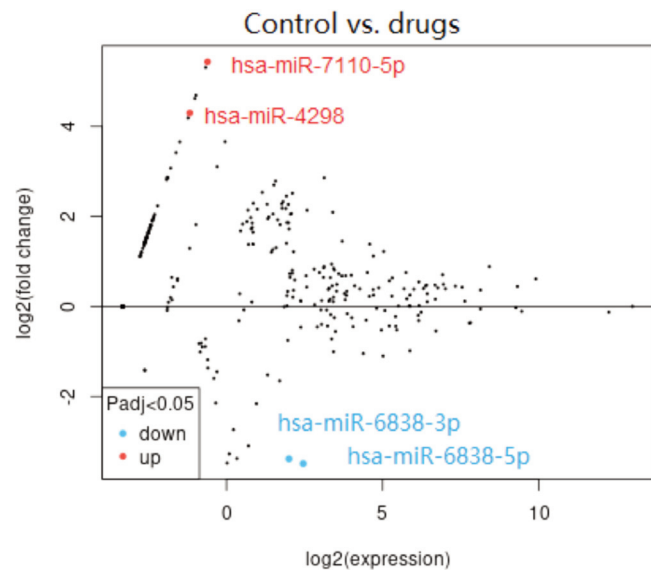


Fig. 4. Differentially expressed miRNAs between untreated CC cell lines and multiple drugs-treated cell lines. RNA sequencing was used to explore differentially expressed miRNAs in non-treated cervical cancer cells (HeLa or SiHa) and cervical cancer cells treated with several anti-tumor extracted components from traditional Chinese Medicine (including emodin, curcumin and Ginsenoside). Intersection of all the data sets of the differentially expressed miRNAs screened. Red color represents significantly upregulated miRNAs in the intersection (higher in control), with log2 fold change >1 (fold change>2) and adjusted P values <0.05, and blue color represents significantly downregulated miRNAs in the intersection (lower in control).

CERS6-AS1 promotes cervical carcinoma progression

revealed that miR-6838-5p inhibitor impeded the CERS6-AS1-knockdown-induced apoptosis (Fig. 6C). Besides, the inhibitory effect of CERS6-AS1-knockdown on the expression of MMP-2 and the promotion effect on the expression of E-cadherin were reversed by miR-6838-5p silencing (Fig. 6E). Taken together, CERS6-AS1 functioned as a sponge of miR-6838-5p to regulate proliferation, invasion and apoptosis of CC cells.

CERS6-AS1 plays a role as a competitive endogenous RNA (ceRNA) in regulating FOXP2 expression by binding to miR-6838-5p

We further explored the molecular mechanism of miR-6838-5p in CC. Based on Starbase analysis, FOXP2 mRNA was found to contain a binding site for miR-6838-5p in 3'UTR (Fig. 7A). RT-qPCR indicated that FOXP2 was distinctly upregulated in C33A, HeLa, SiHa and CaSki cells (Fig. 7B). RIP assay disclosed that miR-6838-5p and FOXP2 coexisted in the anti-Ago2 group

compared with IgG group in HeLa and SiHa cells (Fig. 7C). Luciferase reporter gene assay confirmed that overexpression of miR-6838-5p attenuated luciferase activity of FOXP2-WT, but had no effect on the activity of FOXP2-MUT vector in HeLa and SiHa cells (Fig. 7D). We then transfected miR-6838-5p mimics into HeLa and SiHa cells to evaluate the expression of FOXP2. The result showed that FOXP2 expression was impeded by miR-6838-5p overexpression (Fig. 7E).

To further verify the regulatory effect of CERS6-AS1 and miR-6838-5p on FOXP2, we detected the expression of FOXP2 in HeLa and SiHa cells transfected with CERS6-AS1 siRNA alone or together with miR-6838-5p inhibitor. Western blot results showed that silencing CERS6-AS1 restrained the expression of FOXP2, and miR-6838-5p inhibitor reversed the CERS6-AS1 siRNA-induced FOXP2 downregulation in HeLa and SiHa cells (Fig. 7F). Therefore, the above data revealed that miR-6838-5p interacted directly with FOXP2, and CERS6-AS1 regulated the miR-6838-5p/FOXP2 axis.

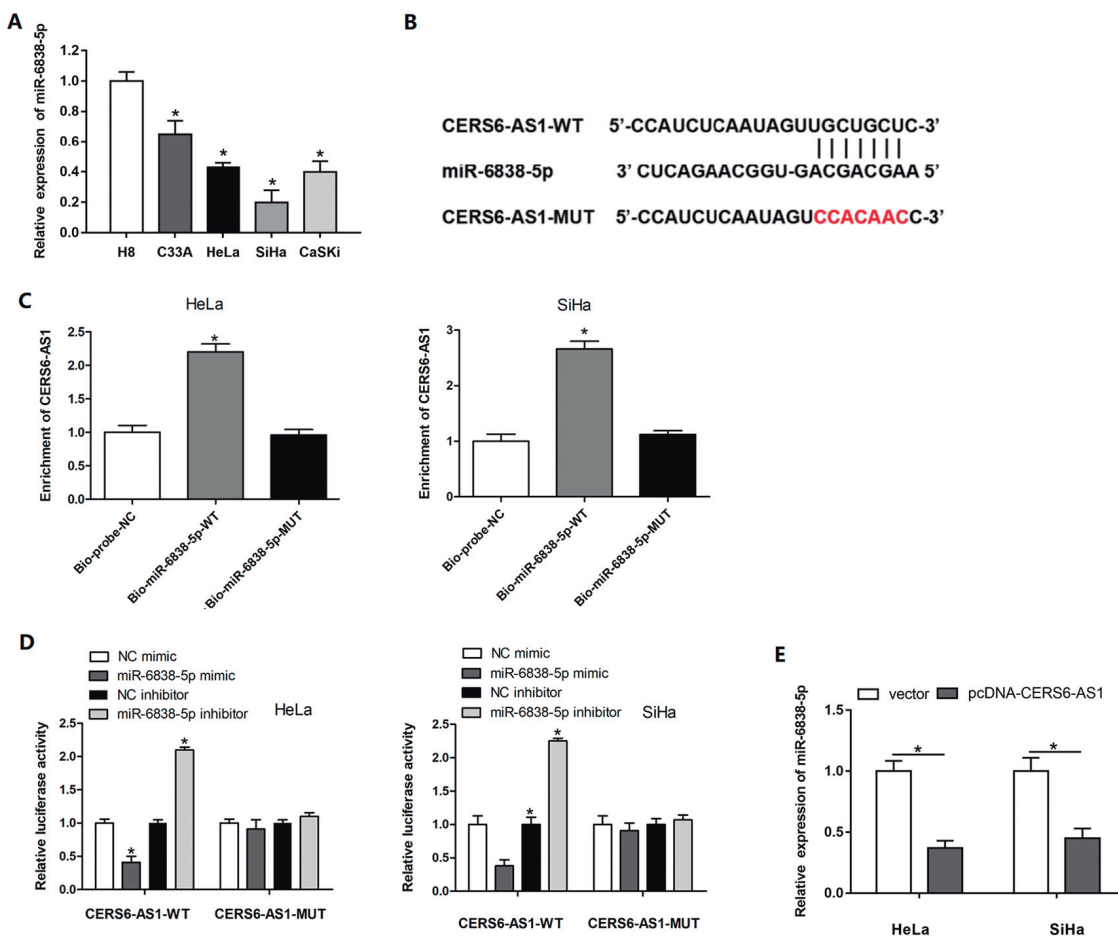


Fig. 5. CERS6-AS1 acted as a sponge of miR-6838-5p. **A.** The expression of miR-6838-5p was detected by RT-qPCR. **B.** The sequences of CERS6-AS1 containing the miR-6838-5p binding sites or mutant binding sites are shown. **C, D.** RNA pull-down and luciferase reporter gene assays were used to detect the interaction between miR-6838-5p and CERS6-AS1 in HeLa and SiHa cells. **E.** The expression of miR-6838-5p was detected in CERS6-AS1-overexpressing HeLa and SiHa cells by RT-qPCR. Data were expressed as mean \pm standard deviation with three replicates. * $P < 0.05$, vs normal human cervical epithelial cells (H8) (A), Bio-probe-NC (C), NC mimic or NC inhibitor group (D), vector or scramble group (E).

CERS6-AS1 promotes cervical carcinoma progression

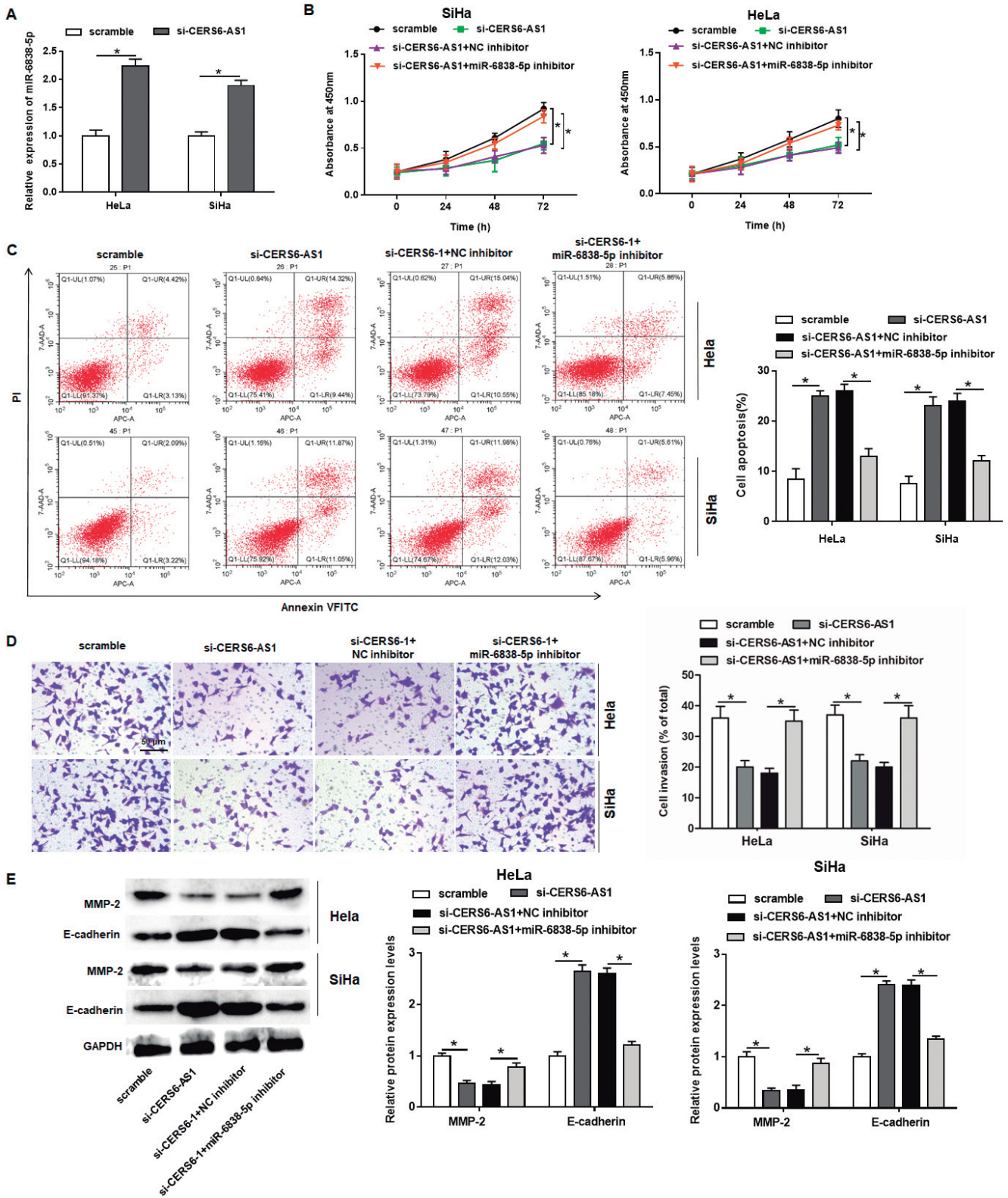


Fig. 6. Effects of miR-6838-5p on the development of CC cells. HeLa and SiHa cells were transfected with CERS6-AS1 siRNA alone or together with miR-6838-5p inhibitor, and incubated for 24h. **A.** The expression of miR-6838-5p was determined by RT-qPCR. **B.** The proliferation ability of HeLa and SiHa cells was detected by CCK-8 assay. **C.** Flow cytometry was performed to assess the apoptosis ratio of transfected cells. **D.** The invasion ability of HeLa and SiHa cells was detected by transwell assay. **E.** The protein level of MMP-2 and E-cadherin were detected by Western blot assay. Data were expressed as mean ± standard deviation with three replicates. **P*<0.05, vs scramble (**A**), scramble or si-CERS6-AS1 + NC inhibitor (**B-E**).

CERS6-AS1 promotes cervical carcinoma progression

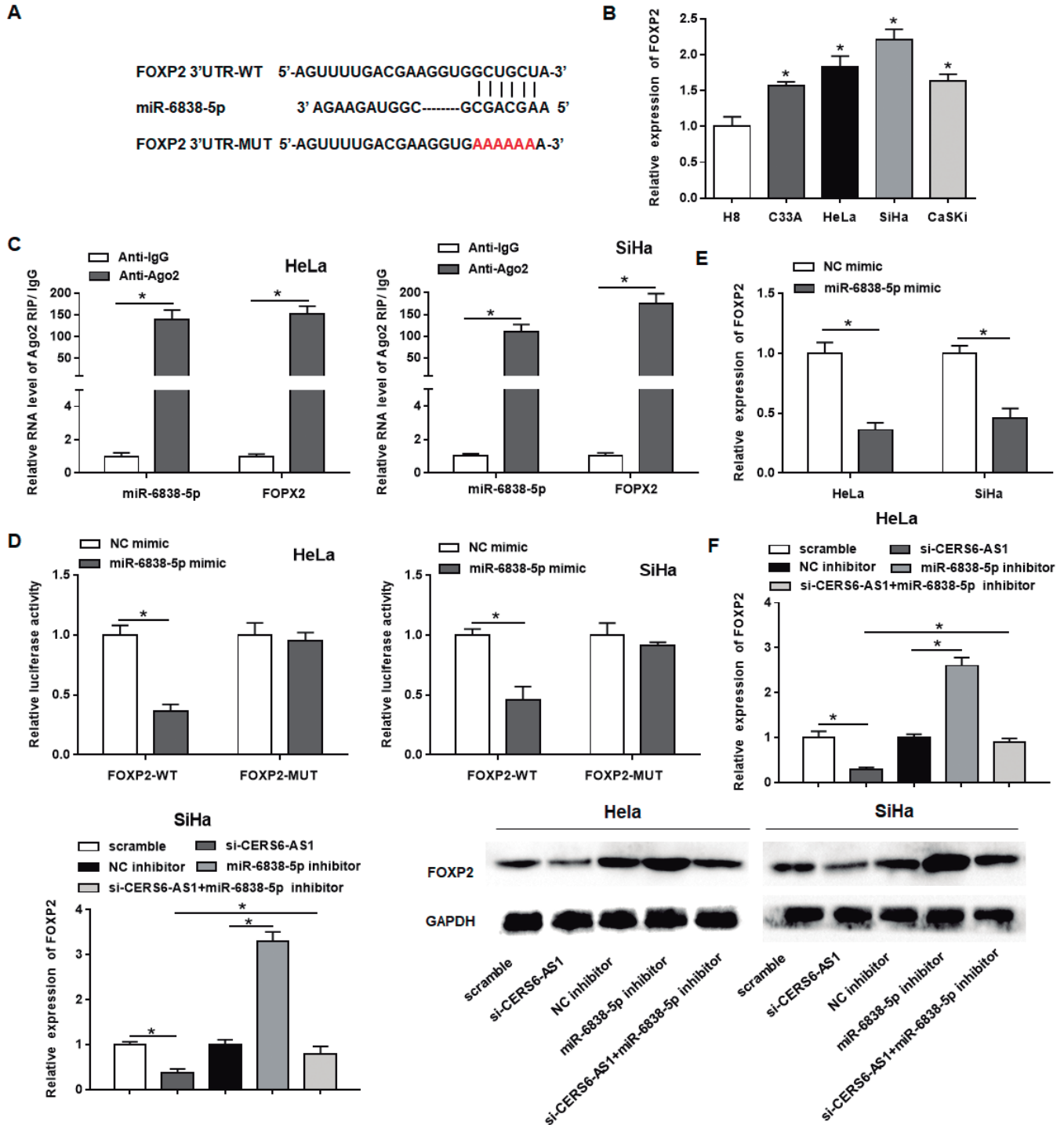


Fig. 7. FOXP2 was targeted by miR-6838-5p. **A.** The sequences of FOXP2 3'UTR containing the miR-6838-5p binding sites or mutant binding sites are shown. **B.** The expression of FOXP2 in CC cell lines was measured by RT-qPCR. **C.** RIP assay was performed to determine the enrichment of miR-6838-5p and FOXP2 in Anti-Ago2 or IgG. **D.** Luciferase reporter gene assay was used to detect the luciferase activities of FOXP2-WT and FOXP2-MUT. **E.** The expression of FOXP2 in transfected HeLa and SiHa cells was examined by RT-qPCR. **F.** Western blot assay was used to detect the expression of FOXP2 protein in HeLa and SiHa cells. Data were expressed as mean \pm standard deviation with three replicates. * P <0.05, vs normal human cervical epithelial cells (H8) (**B**), IgG (**C**), NC mimic (**D**), scramble or NC inhibitor (**E**).

CERS6-AS1 promotes cervical carcinoma progression

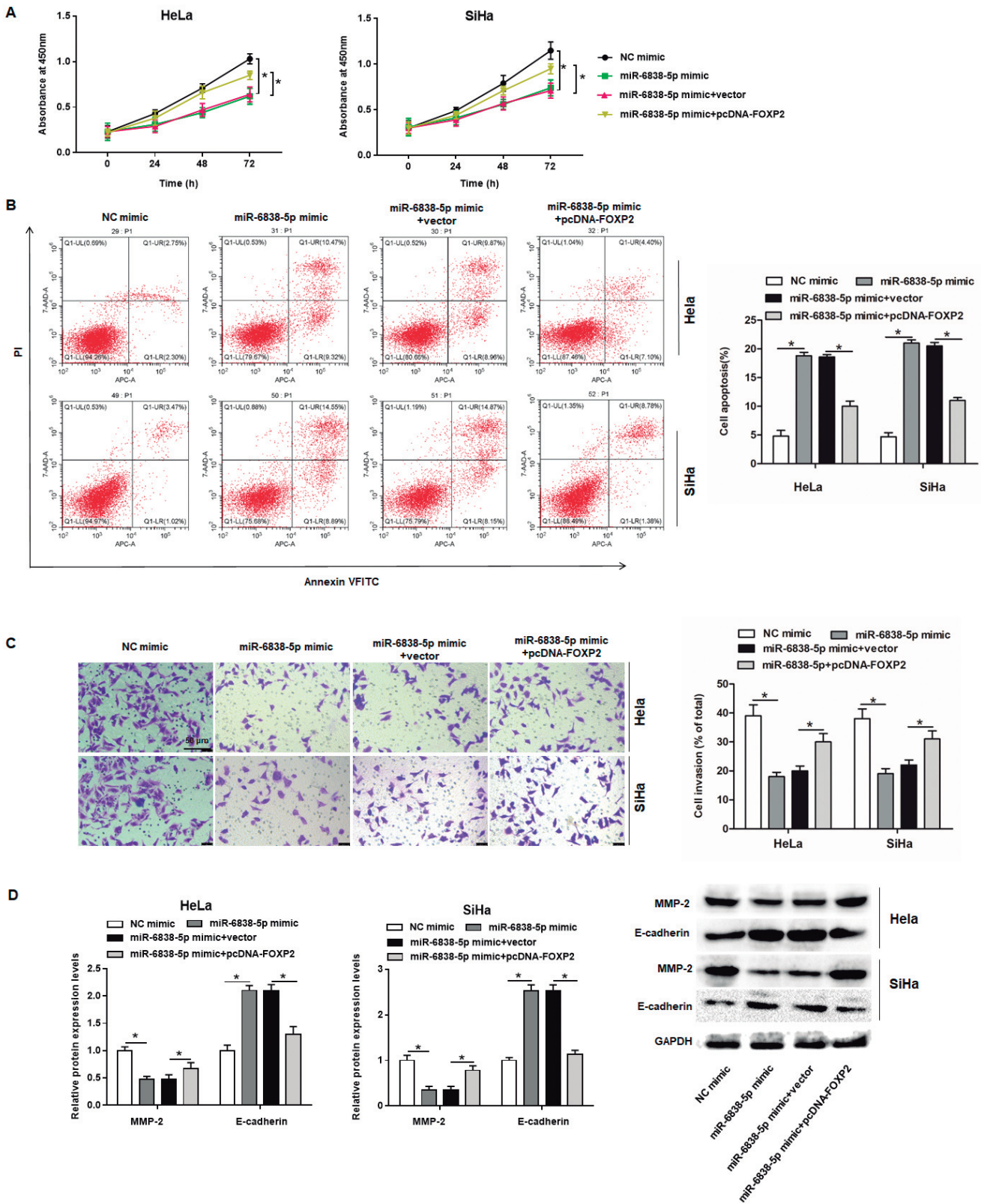


Fig. 8. Effects of FXP2 overexpression on the progression of CC cells. HeLa and SiHa cells were transfected with miR-6838-5p mimic alone or together with pcDNA-FXP2, and incubated for 24h. **A.** The proliferation ability of HeLa and SiHa cells was detected by CCK-8 assay. **B.** Flow cytometry was performed to assess the apoptosis ratio of transfected cells. **C.** The invasion ability of HeLa and SiHa cells was detected by transwell assay. **D.** The protein level of MMP-2 and E-cadherin were detected by Western blot assay. Data were presented as mean \pm standard deviation with three replicates. * $P < 0.05$, vs NC mimic or miR-6838-5p mimic + vector.

The miR-6838-5p/FOXP2 axis affects the malignant behaviors of CC cells

To further investigate whether miR-6838-5p affects the CC cellular fates through FOXP2, HeLa and SiHa cells were transfected with miR-6838-5p mimics alone or together with pcDNA-FOXP2. From the results of CCK-8, we confirmed that the capacity of cell proliferation was decreased by overexpression of miR-6838-5p, which was reversed by FOXP2 overexpression (Fig. 8A). Overexpression of miR-6838-5p markedly inhibited invasion and promoted apoptosis of HeLa and SiHa cells, whereas FOXP2 overexpression inverted these changes (Fig. 8B,C, Fig. 9). Likewise, we also detected the expression of MMP-2 and E-cadherin in HeLa and SiHa cells. The results demonstrated that overexpression of FOXP2 reversed the inhibitory effect of miR-6838-5p mimics on MMP-2 expression and rescued the promotion of miR-6838-5p mimics on E-cadherin expression (Fig. 8D). Thus, these results suggested that overexpression of FOXP2 rescued the miR-6838-5p-mediated proliferation, invasion and apoptosis of CC cells.

Discussion

LncRNAs can regulate gene expression and affect many important physiological processes with a variety of actions, such as chromatin modification factor, X chromosomal inactivation factor, enhancement factor, transcriptional regulation factor and post transcriptional regulation factor (Adnane et al., 2022). They interact with proteins or other classes of RNA molecules, functioning as proto-oncogenes or tumor suppressor genes during cancer progression. LncRNA CERS6-AS1

has been reported to serve as a proto-onco ceRNA to sponge several miRNAs and to upregulate their targeting proto-oncogenes in progression of pancreatic cancer, breast cancer, thyroid cancer and liver cancer (Shen et al., 2021; Yun et al., 2021; Zhao et al., 2022). In this study, we reported that CERS6-AS1 also played a promoting role in the progression of CC in vitro and revealed the underlying mechanism that it served as a sponge of miR-6838-5p to positively regulate the expression of the proto-oncogene FOXP2.

MiRNAs have been proved to be oncogenes or tumor inhibitors involved in regulating progression in various cancers. The pattern of competitive combination between lncRNA and specific miRNA has been found in many studies. The online bioinformatic tool Genecards revealed that miR-6838-5p is negatively associated with the proto-oncogene pathway Wnt/ β -Catenin. As widely recognized, miRNAs functioned through their target genes. Up to date, almost all existing reports have demonstrated that miR-6838-5p targeted a few proto-oncogenes and functions as a tumor suppressor in the progression of some cancers, including gastric, triple-negative breast, osteosarcoma, pancreatic and thyroid cancers (Liu et al., 2019; Zhou et al., 2020; Shen et al., 2021; Liu et al., 2022; Wang et al., 2022). The only exception is that miR-6838-5p targeted the p53 pathway and facilitated cell proliferation and invasion (Zhai et al., 2021). Here, we explored differentially expressed miRNAs in non-treated cervical cancer cells (HeLa or SiHa) and cervical cancer cells treated with several anti-tumor extracted components from traditional Chinese Medicine (including emodin, curcumin and Ginsenoside). Shared miRNAs were screened and the results showed that miR-7110-5p and miR-4298 were the only two miRNAs that are higher in non-treated cells compared with all the treated cell groups, while miR-6838-5p/3p were the only two miRNAs that are lower in non-treated cells compared with all the treated cell groups. We demonstrated that miR-6838-5p was downregulated in CC tissues and cells. Using bioinformatics, luciferase reporter gene and RIP assays, we confirmed that miR-6838-5p was the downstream gene of CERS6-AS1 and was able to bind to CERS6-AS1 to suppress proliferation and invasion, and induce apoptosis of CC cells.

FOXP2 has been reported as a language-related gene and was involved in cancer development. For example, miR-618 was negatively correlated with FOXP2, and overexpression of miR-618 suppressed migration and invasion by directly targeting the FOXP2/TGF- β signaling pathway in prostate cancer (Song et al., 2017). Chen et al. indicated that downregulation of FOXP2 was closely correlated with relapse-free survival, and FOXP2 suppressed breast cancer cell migration and invasion via the TGF- β /SMAD signaling pathway (Chen et al., 2018). In triple-negative breast cancer, FOXP2 was upregulated in triple-negative breast cancer tissues and cell lines, and facilitated tumor growth and metastasis by upregulating GRP78 (Wu et al., 2018). Li et al. reported

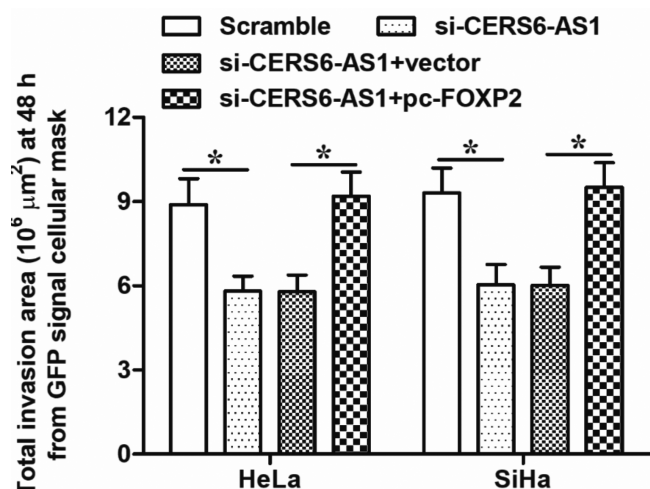


Fig. 9. 3D cell invasion assay was used to evaluate the effect of FOXP2 on overall invasion ability of CC cells. HeLa and SiHa cells were transfected with miR-6838-5p mimic alone or together with pcDNA-FOXP2. 3D cell invasion assay was used to evaluate the overall invasion ability of CC cells. N=4, *P<0.05

that FOXP2 was highly expressed in CC cell lines, and miR-122-5p inhibited FOXP2 expression to promote proliferation and metastasis of CC cells (Li et al., 2019). Our findings indicated that miR-6838-5p was directly targeted at 3'UTR of FOXP2 and also was able to downregulate the expression of FOXP2 in CC. Besides, CERS6-AS1 regulated FOXP2 expression through competitively sponging miR-6838-5p. Interestingly, functional assays confirmed that overexpression of FOXP2 reversed the inhibitory effect of miR-6838-5p mimics on the proliferation and invasion of CC cells.

In conclusion, we revealed that CERS6-AS1 acts as an oncogene to promote CC cell proliferation and invasion, and inhibits apoptosis by acting as a ceRNA that sponges miR-6838-5p to enhance FOXP2 expression. These results demonstrated that the CERS6-AS1/miR-6838-5p/FOXP2 axis is a key player in CC, which may be regarded as a potential therapeutic target for CC.

Data availability statement. The data that support the findings of this study are available from the corresponding author upon reasonable request.

Declaration of conflicting interests. The author(s) declared no potential conflicts of interest with respect to the research, authorship, and/or publication of this article.

Funding. This study was financially supported by the project of Shaanxi Administration of Traditional Chinese Medicine in China (No. 15-LC044) and General Project of Science and Technology Department of Shaanxi Province (No. 2019SF-024) in China.

References

- Adnane S., Marino A. and Leucci E. (2022). LncRNAs in human cancers: Signal from noise. *Trends Cell Biol.* 32, 565-573.
- Bao G., Huang J., Pan W., Li X. and Zhou T. (2020). Long noncoding RNA CERS6-AS1 functions as a malignancy promoter in breast cancer by binding to IGF2BP3 to enhance the stability of CERS6 mRNA. *Cancer Med.* 9, 278-289.
- Bhatla N., Aoki D., Sharma D.N. and Sankaranarayanan R. (2021). Cancer of the cervix uteri: 2021 update. *Int. J. Gynaecol. Obstet.* 155, 28-44.
- Caetano Dos Santos F.L., Wojciechowska U., Michalek I.M. and Didkowska J. (2022). Progress in cancer survival across last two decades: A nationwide study of over 1.2 million polish patients diagnosed with the most common cancers. *Cancer Epidemiol.* 78, 102147.
- Chen M.T., Sun H.F., Li L.D., Zhao Y., Yang L.P., Gao S.P. and Jin W. (2018). Downregulation of FOXP2 promotes breast cancer migration and invasion through TGF β /SMAD signaling pathway. *Oncol. Lett.* 15, 8582-8588.
- D'Oria O., Corrado G., Laganà A.S., Chiantera V., Vizza E. and Giannini A. (2022). New advances in cervical cancer: From bench to bedside. *Int. J. Environ. Res. Public Health* 19, 7094.
- Davies-Oliveira J.C., Smith M.A., Grover S., Canfell K. and Crosbie E.J. (2021). Eliminating cervical cancer: Progress and challenges for high-income countries. *Clin. Oncol.* 33, 550-559.
- Güzel C., van Sten-Van't Hoff J., de Kok I., Govorukhina N.I., Boychenko A., Luider T.M. and Bischoff R. (2021). Molecular markers for cervical cancer screening. *Expert Rev. Proteomics* 18, 675-691.
- Guo H.M., Yang S.H., Zhao S.Z., Li L., Yan M.T. and Fan M.C. (2018). LncRNA NEAT1 regulates cervical carcinoma proliferation and invasion by targeting AKT/PI3K. *Eur. Rev. Med. Pharmacol. Sci.* 22, 4090-4097.
- Huang T., Guan S. and Wang C. (2022). CERS6-AS1 facilitates oncogenesis and restrains ferroptosis in papillary thyroid carcinoma by serving as a ceRNA through miR-497-5p/LASP1 axis. *Ann. Clin. Lab. Sci.* 52, 426-438.
- Li Y., Wang H. and Huang H. (2019). Long non-coding RNA MIR205HG function as a ceRNA to accelerate tumor growth and progression via sponging miR-122-5p in cervical cancer. *Biochem. Biophys. Res. Commun.* 514, 78-85.
- Liu B., Chen J., Shang F., Lian M., Shen X. and Fang J. (2022). Tumor-derived exosome FGD5-AS1 promotes angiogenesis, vascular permeability, and metastasis in thyroid cancer by targeting the miR-6838-5p/VAW2 axis. *J. Oncol.* 2022, 4702855.
- Liu G., Wang P. and Zhang H. (2019). MiR-6838-5p suppresses cell metastasis and the EMT process in triple-negative breast cancer by targeting WNT3A to inhibit the Wnt pathway. *J. Gene Med.* 21, e3129.
- Peng W.X., Koirala P. and Mo Y.Y. (2017). LncRNA-mediated regulation of cell signaling in cancer. *Oncogene* 36, 5661-5667.
- Shen R., Wang X., Wang S., Zhu D. and Li M. (2021). Long noncoding RNA CERS6-AS1 accelerates the proliferation and migration of pancreatic cancer cells by sequestering microRNA-15a-5p and microRNA-6838-5p and modulating HMGA1. *Pancreas* 50, 617-624.
- Song X.L., Tang Y., Lei X.H., Zhao S.C. and Wu Z.Q. (2017). MiR-618 inhibits prostate cancer migration and invasion by targeting FOXP2. *J. Cancer* 8, 2501-2510.
- Volkova L.V., Pashov A.I. and Omelchuk N.N. (2021). Cervical carcinoma: Oncobiology and biomarkers. *Int. J. Mol. Sci.* 22, 12571.
- Wang F., Sun H., Li K., Yang K., Xiang Y. and Tian X. (2022). CircRASSF2 promotes IGF1R and osteosarcoma metastasis via sponging miR-6838-5p. *Ann. Transl. Med.* 10, 11.
- Wu J., Liu P., Tang H., Shuang Z., Qiu Q., Zhang L., Song C., Liu L., Xie X. and Xiao X. (2018). FOXP2 promotes tumor proliferation and metastasis by targeting GRP78 in triple-negative breast cancer. *Curr. Cancer. Drug. Targets* 18, 382-389.
- Yun Z., Meng F., Li S. and Zhang P. (2021). Long non-coding RNA CERS6-AS1 facilitates the oncogenicity of pancreatic ductal adenocarcinoma by regulating the microRNA-15a-5p/FGFR1 axis. *Aging (Albany NY)*. 13, 6041-6054.
- Zhai X., Wu Y., Zhang D., Li H., Chong T. and Zhao J. (2021). MiR-6838-5p facilitates the proliferation and invasion of renal cell carcinoma cells through inhibiting the DMTF1/ARF-p53 axis. *J. Bioenerg. Biomembr.* 53, 191-202.
- Zhang J. and Lou W. (2020). A key mRNA-miRNA-lncRNA competing endogenous RNA triple sub-network linked to diagnosis and prognosis of hepatocellular carcinoma. *Front. Oncol.* 10, 340.
- Zhang J., Yao T., Wang Y., Yu J., Liu Y. and Lin Z. (2016). Long noncoding RNA MEG3 is downregulated in cervical cancer and affects cell proliferation and apoptosis by regulating miR-21. *Cancer Biol. Ther.* 17, 104-113.
- Zhao S.Y., Wang Z., Wu X.B., Zhang S., Chen Q., Wang D.D. and Tan Q.F. (2022). CERS6-AS1 contributes to the malignant phenotypes of

CERS6-AS1 promotes cervical carcinoma progression

- colorectal cancer cells by interacting with miR-15b-5p to regulate SPTBN2. *Kaohsiung J. Med. Sci.* 38, 403-414.
- Zhou Y., Xu Z., Yu Y., Cao J., Qiao Y., Qiao H. and Suo G. (2019). Comprehensive analysis of the lncRNA-associated ceRNA network identifies neuroinflammation biomarkers for Alzheimer's disease. *Mol. Omics* 15, 459-469.
- Zhou W., Ding X., Jin P. and Li P. (2020). MiR-6838-5p affects cell growth, migration, and invasion by targeting gprin3 via the Wnt/ β -catenin signaling pathway in gastric cancer. *Pathobiology* 87, 327-337.

Accepted November 29, 2022